Chemical Physics Letters 706 (2018) 285–294

Contents lists available at ScienceDirect

Chemical Physics Letters

journal homepage: www.elsevier.com/locate/cplett

Molecular modeling the adsorption behavior of bone morphogenetic protein-2 on hydrophobic and hydrophilic substrates

Izabele Marquetti [a], Salil Desai [a,b,*]

[a] Department of Industrial & Systems Engineering, North Carolina A&T State University, Greensboro, NC 27411, USA
[b] Wake Forest Institute for Regenerative Medicine, Wake Forest School of Medicine, Winston–Salem, NC 27157, USA

ARTICLE INFO

Article history:
Received 17 May 2018
In final form 9 June 2018
Available online 12 June 2018

Keywords:
Bone morphogenetic protein-2
Gold
Molecular dynamics
Protein adsorption
Silicon nitride

ABSTRACT

Adsorption of BMP-2 on hydrophobic gold and hydrophilic silicon nitride is studied using molecular dynamics simulations. The wetting behavior of the dissolution media directly guided the protein-substrate interaction, impacting the protein adsorption. The saline solution restricted the movement of the protein on gold, limiting adsorption to hydrophobic and charged residues while preserving the secondary structure. Stronger adsorption occurred on silicon nitride where the protein had more flexibility to interact with the surface leading to the disruption of β-sheet structures in two orientations. This research contributes to the understanding of BMP-2 adsorption behavior in four orthogonal orientations with medically relevant materials.

© 2018 Elsevier B.V. All rights reserved.

1. Introduction

Protein adsorption onto substrates is an important phenomenon in biotechnology due to its influence in the biocompatibility of implants and the effectiveness of engineered tissue scaffolds for cellular differentiation and proliferation [1,2]. The protein-substrate interactions are vital in preserving the biological response of the proteins [3]. The properties of the substrate surface, including wetting properties, crystal orientation, and topology, regulate the final conformation and bioactivity of the adsorbed protein [4]. Protein structure can change from its native state to an unfolded configuration depending on the surface characteristics, which can lead to partial denaturation of the protein [3,5].

Bone morphogenetic protein-2 (BMP-2) is an essential protein for bone formation and restoration because of its potential to promote differentiation and proliferation of osteoblasts [6]. BMP-2 combined with standard methods for bone repair can reduce the healing time and risk of rejection, allowing savings in the treatment cost. However, its use for clinical procedures requires the protein to be incorporated in a carrier agent without significant conformational changes to maintain its bioactivity [7]. For the effective bone development, BMP-2 adsorption on the implant surface must be stable and occur exclusively on the implant site. Also, the protein must interact with its receptors to activate signaling cascades, inducing osteoblasts proliferation [3]. Partial denaturation of the protein can occur if the binding to the surface is too strong which directly affects the protein bioactivity. Therefore, a balance between steady adsorption on the substrate and conservation of protein activity must be achieved [3]. BMP delivery at the affected site relies on media pH, substrate porosity, temperature, the salt concentration of the solute, and the interaction between substrate and protein [8]. Therefore, its retention depends if the growth factor is immobilized on the substrate during manufacturing or absorbed into the substrate [8].

The interaction between protein and substrate at the nanoscale depends on different surface parameters, including chemical composition, charge, topography, and hydrophilicity, which influence protein conformation, adsorption, and bioactivity [9]. Proteins interact with a substrate through intramolecular bonds, including hydrophobic interactions, ionic bonds, and charge transfer. Hydrophilicity of substrates is a critical parameter for the adsorption of proteins. Usually, hydrophilic surfaces adsorb fewer proteins than hydrophobic [10]. However, protein adsorption also depends on the properties of the amino acids that form a protein. Amino acids are classified as charged, polar and hydrophobic. Charged residues are highly exposed to solvents, often forming salt bridges which influence the stability of proteins [11]. Hydrophobic amino acids residues tend to adsorb on hydrophobic substrates, whereas polar residues on hydrophilic substrates [10].

Different substrate materials with medical relevance, such as gold [12], graphite [3,13], and hydroxyapatite [9,14] have been

* Corresponding author at: Department of Industrial & Systems Engineering, North Carolina A&T State University, Greensboro, NC 27411, USA.
E-mail address: sdesai@ncat.edu (S. Desai).

https://doi.org/10.1016/j.cplett.2018.06.015
0009-2614/© 2018 Elsevier B.V. All rights reserved.

studied to understand their interaction with proteins. In recent years, a new class of materials which include silicon nitride [15] and silicon dioxide [16] have been used for orthopedic applications due to their improved biocompatibility. Gold has been widely used as a substrate material because of its optical, magnetic, and chemical properties, with applications in biological imaging, drug delivery system and biosensors [12]. Silicon nitride has been used in spinal surgery for bone fusion and to extend the durability of prosthetic hip and knee joints [15]. However, the interaction of proteins with these materials needs further exploration for their effective implementation in clinical settings.

Molecular modeling can be used to visualize better, understand and predict the interaction between proteins and material surfaces to control cellular function [1,2]. Studies of 3D protein structures are essential to understanding the BMP-2 release kinetics for orthopedic applications [17]. The benefits of BMPs in the regeneration of bone tissue are well-known and studied in the medical field [18–20]. However, the effective release of this protein at tissue-implant interface needs further investigation. Understanding how ambient conditions affect the release kinetics of BMP-2 on different substrate materials and morphologies will progress the field of orthopedics. Successful coatings of BMP-2 on implants might reduce the cases of rejection and avoid infections, significantly reducing the recovery time of bone and cartilage injuries [6]. Current clinical practices employ BMP-2 growth factors at implant site with mixed results [21]. Growth factors are typically sensitive to ambient *in vivo* environments and susceptible to denaturation [22]. Also, prolonged retention is required to maintain the properties of growth factors in the cells, artificial scaffolds, or extracellular matrix [23]. Thus, it is critical that the molecular mechanisms for the adsorption kinetics and bioactivity of BMP-2 be studied to direct cell-specific differentiation and proliferation. Our research group implements MD simulations to investigate BMP-2 growth factor in four initial orientations concerning substrate materials based on their varying wetting behaviors. The hydrophobic and hydrophilic characteristics are represented by gold and silicon nitride (Si_3N_4) substrate materials, respectively.

2. Methods

The MD simulations were performed on a 64-bit Linux platform (Fedora 21) with two graphical processing units (GPUs) from NVIDIA® Corporation (K40 and K20, with 2880 and 2496 cores, respectively). Nanoscale Molecular Dynamics (NAMD) source code version 2.11 was implemented to execute the simulations with CHARMM27 force field [24]. Visual Molecular Dynamics (VMD) platform was used to create the molecular models and analyze the results [25]. The Theoretical and Computational Biophysics Group at Beckman Institute for Advanced Science and Technology at the University of Illinois at Urbana-Champaign developed both NAMD and visual MDs [25].

A BMP-2 protein representation (PDB: 3BMP) was obtained from the RCSB Protein Data Bank [26]. The BMP-2 molecule consisted of 1641 atoms, with 1664 bonds, at 2.7 Å resolution. An explicit TIP3P water model was used to solvate the protein in a minimum water sphere [27], and then, sodium chloride (NaCl) ions were added using VMD plugin at a concentration of 0.15 mol/L. This solvated aqueous protein model consisted of a 6.5 nm droplet with 13,863 atoms. Non-bulk models have been successfully used to study protein conformation [3,5,28].

For modeling the interaction of the substrate with the droplets, the solvated protein was placed tangent on the center of a flat

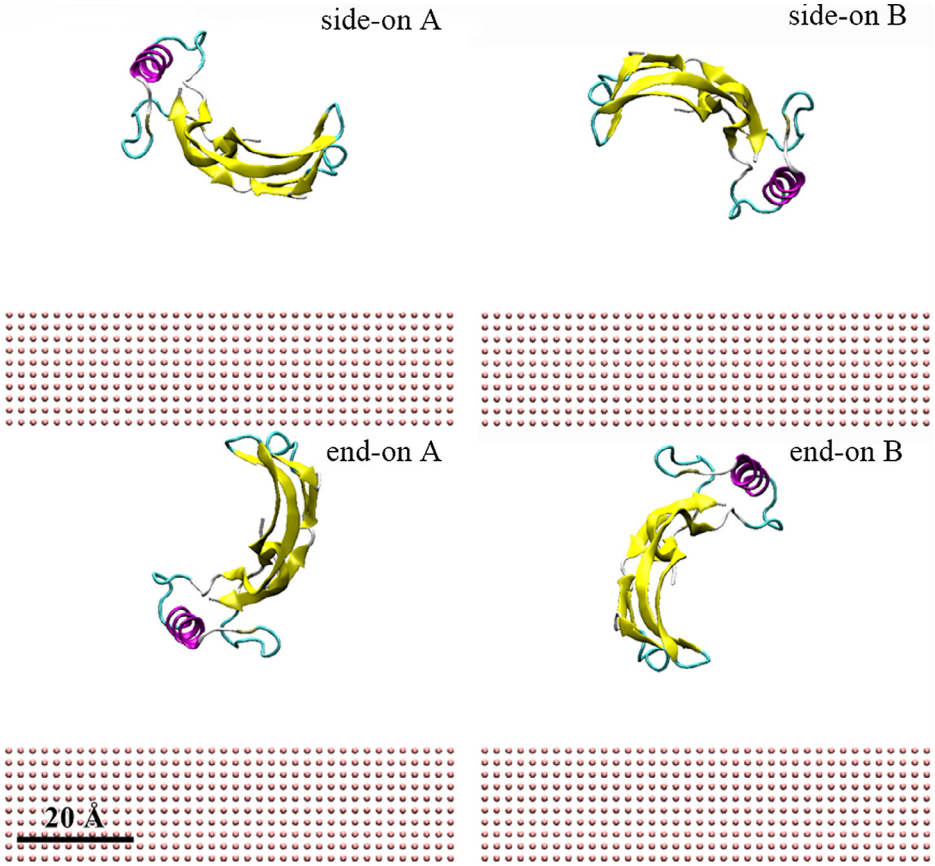

Fig. 1. Initial orientations of BMP-2 on hydrophobic gold (same orientations considered for silicon nitride). Protein is represented using secondary structure, α-helix is represented in pink and β-sheets in yellow. (For interpretation of the references to color in this figure legend, the reader is referred to the web version of this article.)

substrate. The initial orientation of the protein influences the protein-surface interactions due to the special characteristics (hydrophobic, hydrophilic and charged) [29] of the amino acids that form the BMP-2. For this reason, we considered four different initial orientations of the protein, two side-on and two end-on (see Fig. 1). Gold and silicon nitride substrates were constructed using VMD plugin with dimensions of 200 × 200 × 20 Å and 320 × 200 × 20 Å, respectively.

The bonded and non-bonded parameters for water molecules and protein were obtained from the CHARMM force fields [30]. The non-bonded force field parameters used in the simulations for gold were σ_{ij} = 3.694 Å and ϵ_{ij} = −0.163 kJ/mol [31], and for silicon nitride σ_{ij}(Si) = 4.270 Å, ϵ_{ij}(Si) = −1.297 kJ/mol, σ_{ij}(N) = 3.995 Å, and ϵ_{ij}(N) = −0.795 kJ/mol [32].

All simulations were minimized for 0.2 ns and performed for 20 ns with a 2 fs integration time step. Data were recorded every 0.1 ns. The cutoff distance for Van der Waals interactions was 12 Å. Periodic boundary condition was applied for x- and y- directions. The systems were simulated at a constant temperature of 310 K using Langevin temperature control [33]. All the atoms in the substrate were fixed.

3. Results and discussion

The effects of the protein orientations and substrate materials on the protein adsorption were evaluated over time. Fig. 2 shows the side-on A orientation on gold and silicon nitride substrates with equilibrium contact angles of 121° [34,35] and 35° [36,37]

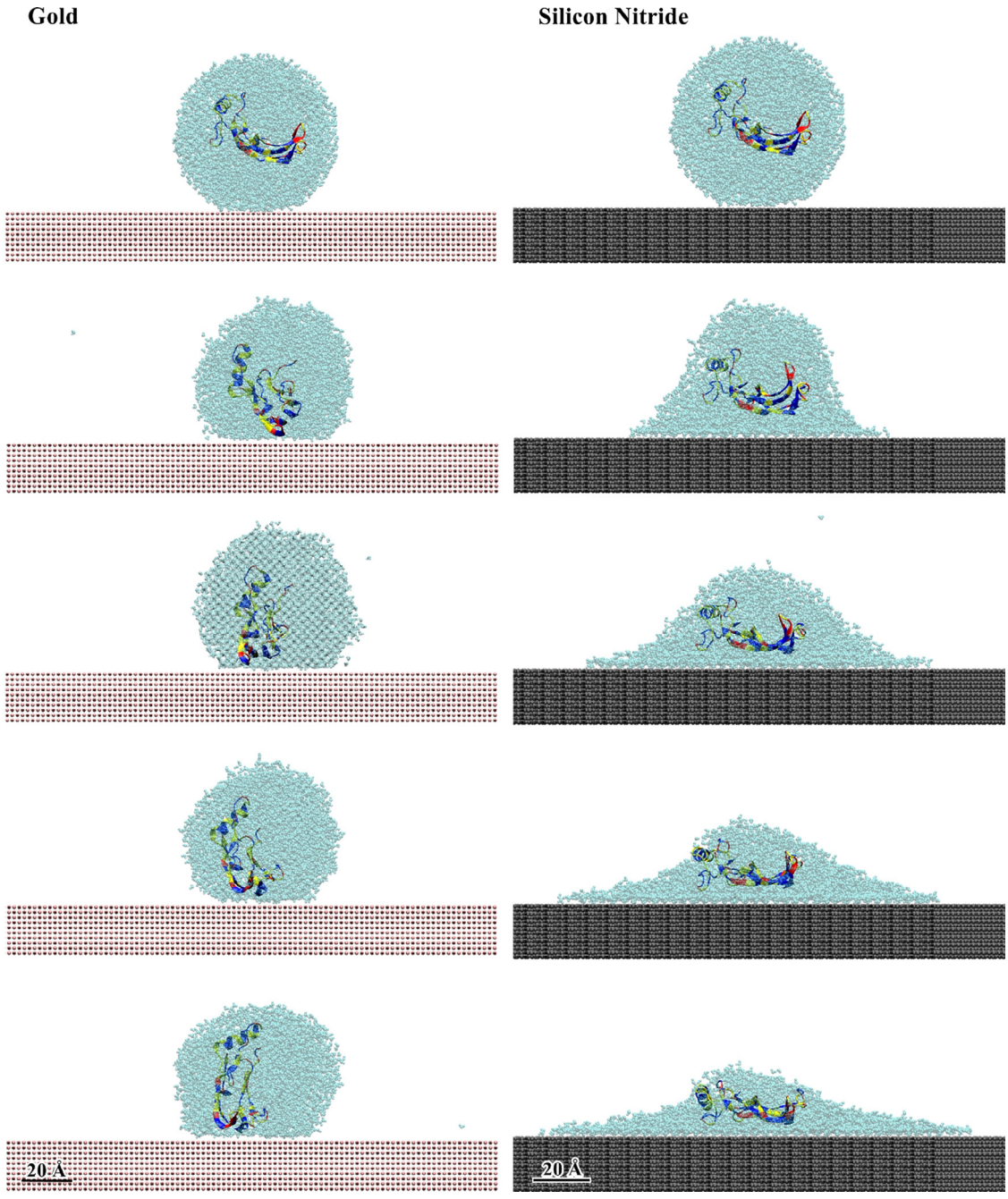

Fig. 2. Side view of droplets spreading over time. Protein (side-on A orientation) is represented according to the characteristics of the residues; charged amino acids are shown in red, polar in yellow, and hydrophobic in blue. (For interpretation of the references to color in this figure legend, the reader is referred to the web version of this article.)

representing hydrophobic and hydrophilic interactions, respectively. The wetting behavior of the substrates directly affects the behavior of the protein along with the presence of salt ions, which can create a barrier that prevents adsorption. In hydrophobic gold, the solvent restricted the movement of the protein avoiding the contact of most residues with the substrate, and only a few charged and hydrophobic residues could adsorb.

On the contrary, simulations using hydrophilic silicon nitride allowed the protein to have a stronger interaction with the substrate. This is because the solvent pulled the protein towards the substrate during the spreading phase, allowing a higher number of protein atoms to be available for adsorption. These findings contradict the fact that hydrophobic materials usually tend to adsorb more proteins and hydrophilic materials have a certain resistance to protein adsorption [10]. This contrary behavior might be related to the presence of a dissolution media which has a high influence on protein adsorption. Polar amino acids in the protein are attracted to the water molecules, which prevents the protein from having some of its charged and hydrophobic residues to interact with the gold substrate. On the other hand, protein adsorption is highly favorable on silicon nitride because the solvent allows the protein to spread out more on the surface, making more residues available to adsorb. Thus, the adsorption of protein is a function of the three-way interaction between the protein, the dissolution media (NaCl 0.15 mol/L water) and the substrate.

The structural stability of the protein models was evaluated using the root-mean-square-deviation (RMSD) of the atomic coordinates. For the models simulated on hydrophobic gold, the initial orientation influenced the average values of RMSD, presenting fluctuations in the values (see Fig. 3(a)). In the models simulated with hydrophilic silicon nitride, only small changes occurred on the RMSD values and equilibration was reached for all the orientations at approximately 3 ns (see Fig. 3(b)).

According to Utesch et al. [3], the adsorption of BMP-2 onto the surface of the substrate can be measured by the adsorption energy. This can be quantified as the number of contacts, which is the number of atoms in a residue that are within 5 Å of the substrate. Protein adsorption energy was measured by the non-bonded interaction energies. These include both the Van der Waals and electrostatic energies of the interaction between protein and substrate. The strength of interaction depends on the type of interaction forces. Van der Waals interactions are very weak (energy less than 50 kJ/mol) while electrostatic interactions are strong (energy higher than 100 kJ/mol) [38].

The adsorption of BMP-2 on gold is significantly different from the adsorption on silicon nitride. In all simulations using gold as a substrate, the electrostatic energy is zero, and the adsorption energy corresponds only to the Van der Waals energy, confirming that interactions between protein and gold are usually weak [12]. For these simulations, BMP-2 adsorption occurred within less than 2 ns for side-on B and end-on B. Simulation with end-on A initial orientation took the longest time to initiate adsorption (14 ns). However, adsorption was stronger as compared to other simulations (see Fig. 4(a)). On almost all systems, except end-on A

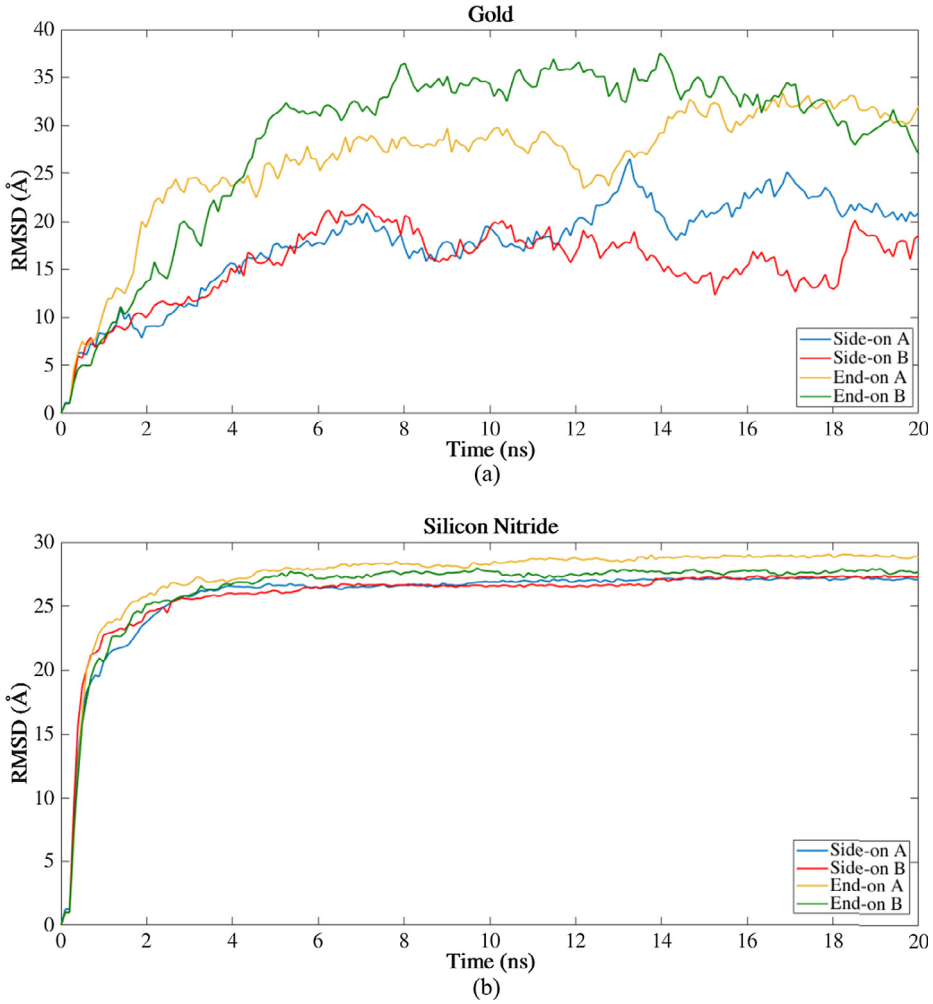

Fig. 3. Root-mean-square-deviation as a function of time for protein models on (a) gold and (b) silicon nitride.

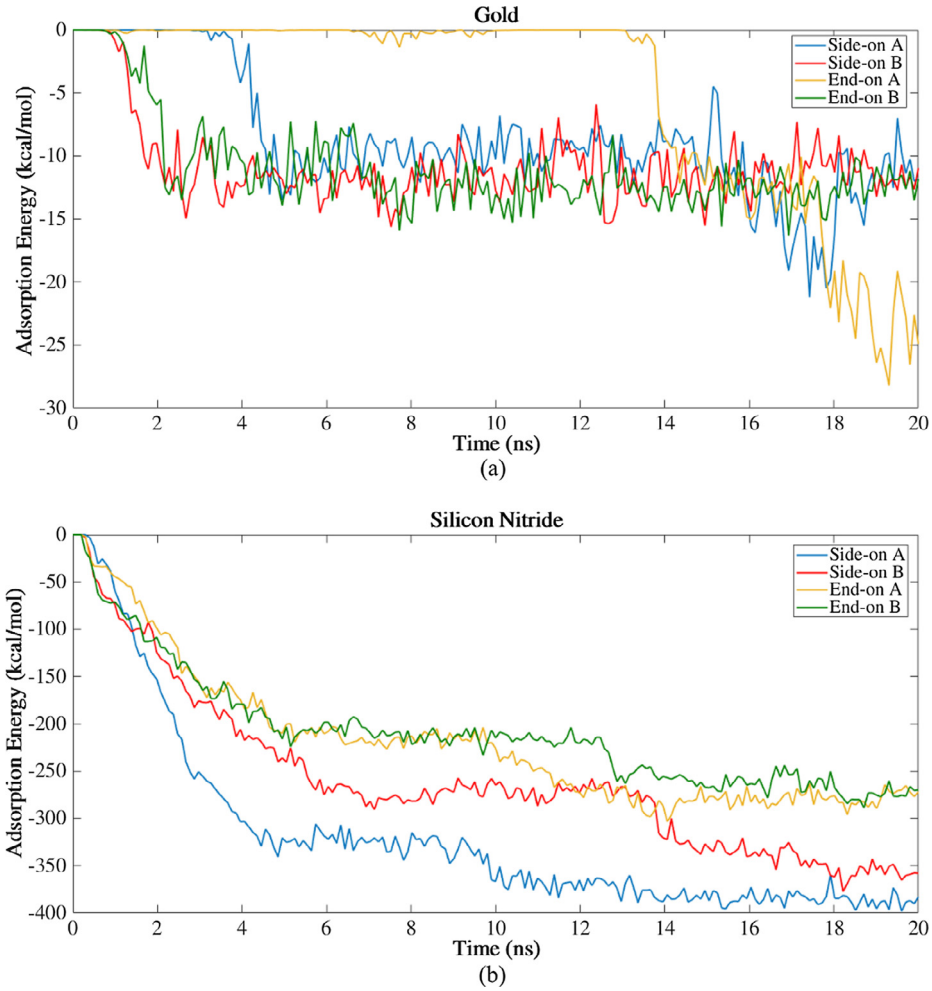

Fig. 4. Adsorption energy of protein with (a) gold and (b) silicon nitride substrate.

orientation, the protein adsorbed with a perpendicular orientation towards the surface, which was influenced by the arrangement of salt ions during the simulations. For the simulations performed with hydrophilic silicon nitride, similar adsorption behavior occurred for all initial orientations considered. All simulations stabilize at 5 ns but stronger adsorption occurred for side-on A and B (see Fig. 4(b)). The water molecules formed a layer between protein and surface. This is consistent with findings for hydrophilic substrates where proteins do not have direct contact with the surface and are involved in a constrained water layer [39]. According to Kyriakides [40], even though the arrangement of water molecules on the surface of a hydrophilic substrate can be a barrier to protein adsorption, charge interactions and conformational changes of the protein can promote adsorption processes due to favorable energetic changes.

The radius of gyration of the BMP-2 was calculated to analyze the compaction level that occurred in its structure during each simulation. This measure was used to evaluate the protein unfolding behavior. For the simulations performed on gold, all the orientations presented similar compaction behavior, preserving the initial structure (see Fig. 5(a)). This might be related with the fact that the solvent restrained the movement of the protein on the gold substrate. The end-on A configuration had less flexibility for spreading which explains its late adsorption behavior. For the simulations performed using silicon nitride as a substrate, the initial orientation influences the unfolding behavior of the protein. Simulations performed with side-on A configuration spread completely forming a layer on the substrate (Fig. 5(b)). This is evident with its high radius of gyration and corresponding highest adsorption energy (−1500 kJ/mol). The end-on A configuration presented steady secondary structures with lower values of radius of gyration on both Si_3N_4 and gold substrates. This behavior confirms that the end-on A orientation has less flexibility for unfolding on the substrates.

Protein denaturation was evaluated by comparing the secondary structure of each configuration between the initial and final conformation. Denaturation disrupts the α-helix and β-sheet structures transforming them into a random coil state [41]. Higher conformational changes in the secondary structures occurred for the simulations performed on silicon nitride as compared to gold (see Table 1). The silicon nitride substrate had minimal changes to the α-helix structures in most of the simulations. Side-on B and end-on B configurations had significant losses of β-sheet structure. This loss of secondary structure is in agreement with a similar MD study of protein adsorption conducted by Mücksch et al. [4]. They revealed that the hydrophilic substrate greatly disturbed the secondary structure of the streptavidin protein as compared to the hydrophobic substrate. Based on this partially denatured protein structure on silicon nitride substrate, cascading interactions with Type I and Type II cell receptors seem unlikely. Thus, we conclude that the side-on B and end-on B orientations in a BMP-2 monomer configuration may not be suitable for coating a hydrophilic substrate such as silicon nitride.

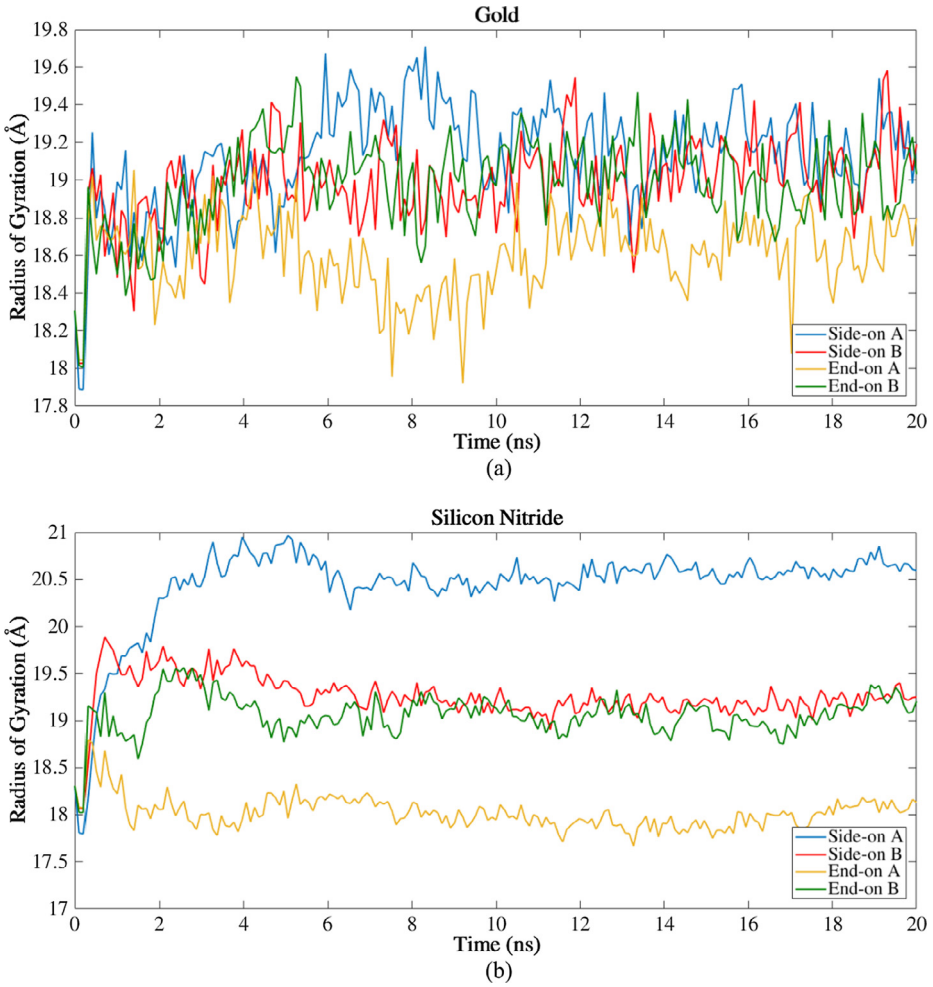

Fig. 5. Evolution of the radius of gyration of BMP-2 over time for simulations performed on (a) gold and (b) silicon nitride.

Table 1
Initial and final secondary structure of BMP-2 on gold and silicon nitride substrates.

SS	Initial structure (%)	After 20 ns (%)							
		Gold				Silicon nitride			
		Side-on A	Side-on B	End-on A	End-on B	Side-on A	Side-on B	End-on A	End-on B
α-helix	10.38	11.32	12.26	10.38	11.32	9.43	14.15	7.55	10.38
3_{10}-helix	0.00	0.00	2.83	0.00	0.00	0.00	2.83	2.83	6.60
β-sheet	44.34	40.57	44.34	44.34	42.45	42.45	31.13	41.51	32.08

Figs. 6 and 7 show the number of contacts between residue atoms and substrate within a distance of 5 Å. Residues were selected based on their higher contributions to the adsorption behavior with the substrate. For hydrophobic gold, most of the adsorbed residues were charged or hydrophobic. The side-on A orientation had at most 99 atoms in a residue contacting the substrate, which was the highest number for the gold substrate. Different VAL and LEU residue chains adsorbed in all orientations simulated. Fig. 7 shows that a higher number of residue atoms adsorbed on hydrophilic silicon nitride, reaching 219 atoms for end-on A orientation. The residues with greater number of contacts (greater than 120) were mostly charged, including ARG, GLU, and LYS. The other adsorbed amino acids included different residues, both polar and hydrophobic.

For the gold substrate, the solvent interfered with the adsorption phenomena and only hydrophobic and charged residues that were exposed on the surface of the drop adsorbed on the surface. Consequently, contributing to the weaker adsorption on gold as compared to silicon nitride. Moreover, the non-wetting hydrophobic drop restricted the movement of the protein, thereby preserving its secondary structure in all orientations on the gold substrate. The side-on orientations for both substrates had more atoms interacting with the surface. Hydrophobic LEU100, VAL98, and LEU90 were the main residues adsorbing on the surface in side-on A orientation, while charged LYS73 and hydrophobic VAL63, VAL67 and VAL70 adsorbed in side-on B orientation (see Fig. 8). Charged LYS97 strongly adsorbs at 4 ns, but desorbed after 6 ns. This confirms the fact that hydrophobic amino acid residues tend to adsorb on hydrophobic substrate [10]. The cysteine knot structure was retained providing structural stability for the BMP-2 monomer without its hydrophobic core [42]. Both the

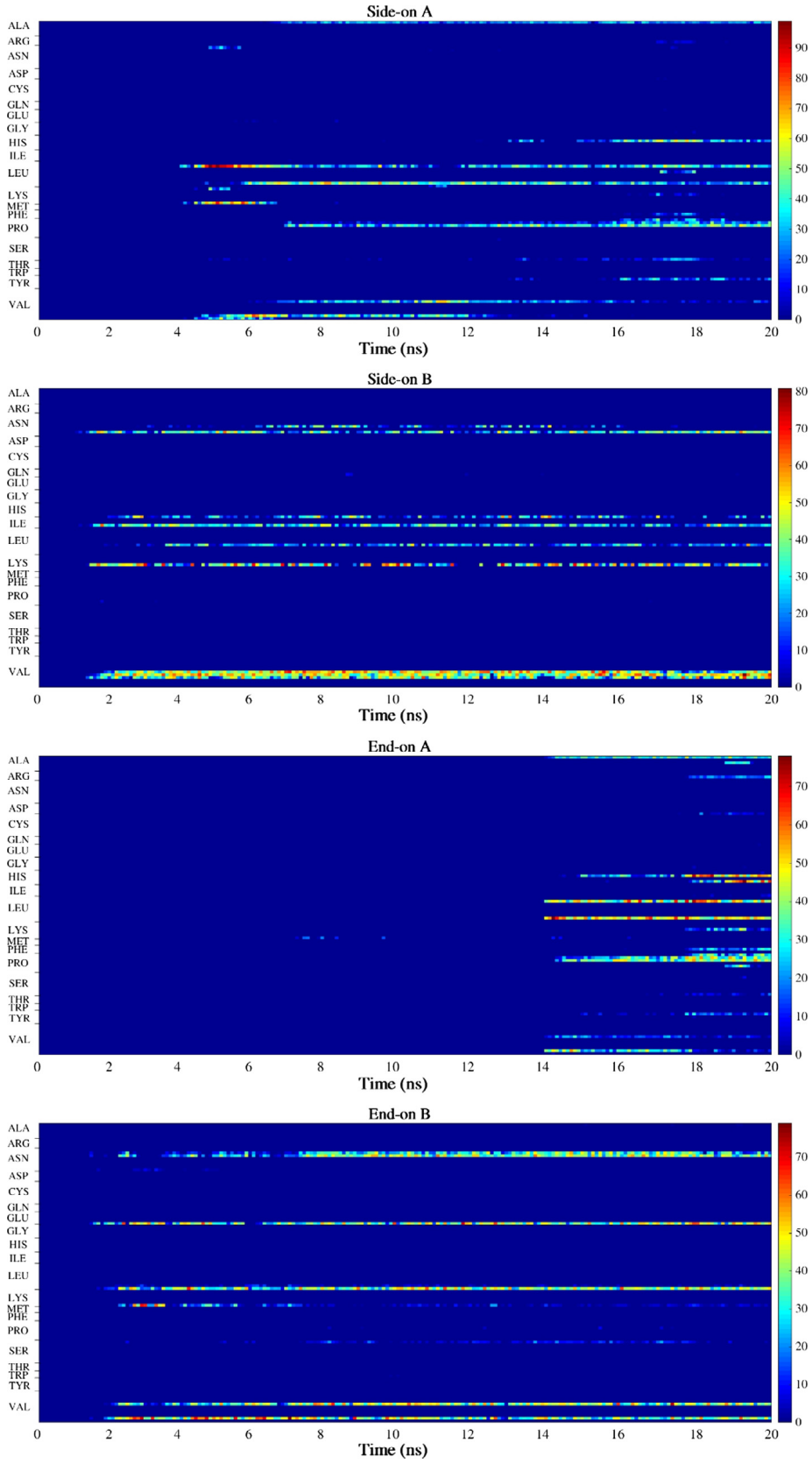

Fig. 6. Number of contacts between residue atoms and gold substrate during 20 ns simulations.

wrist and knuckle epitopes were conserved after the adsorption of BMP-2 on gold providing signaling pathways to Type I and Type II receptors, respectively [43]. These receptors activate a signaling cascade within the cell through the SMAD pathway initiating chondrogenesis towards bone morphogenesis [44,45].

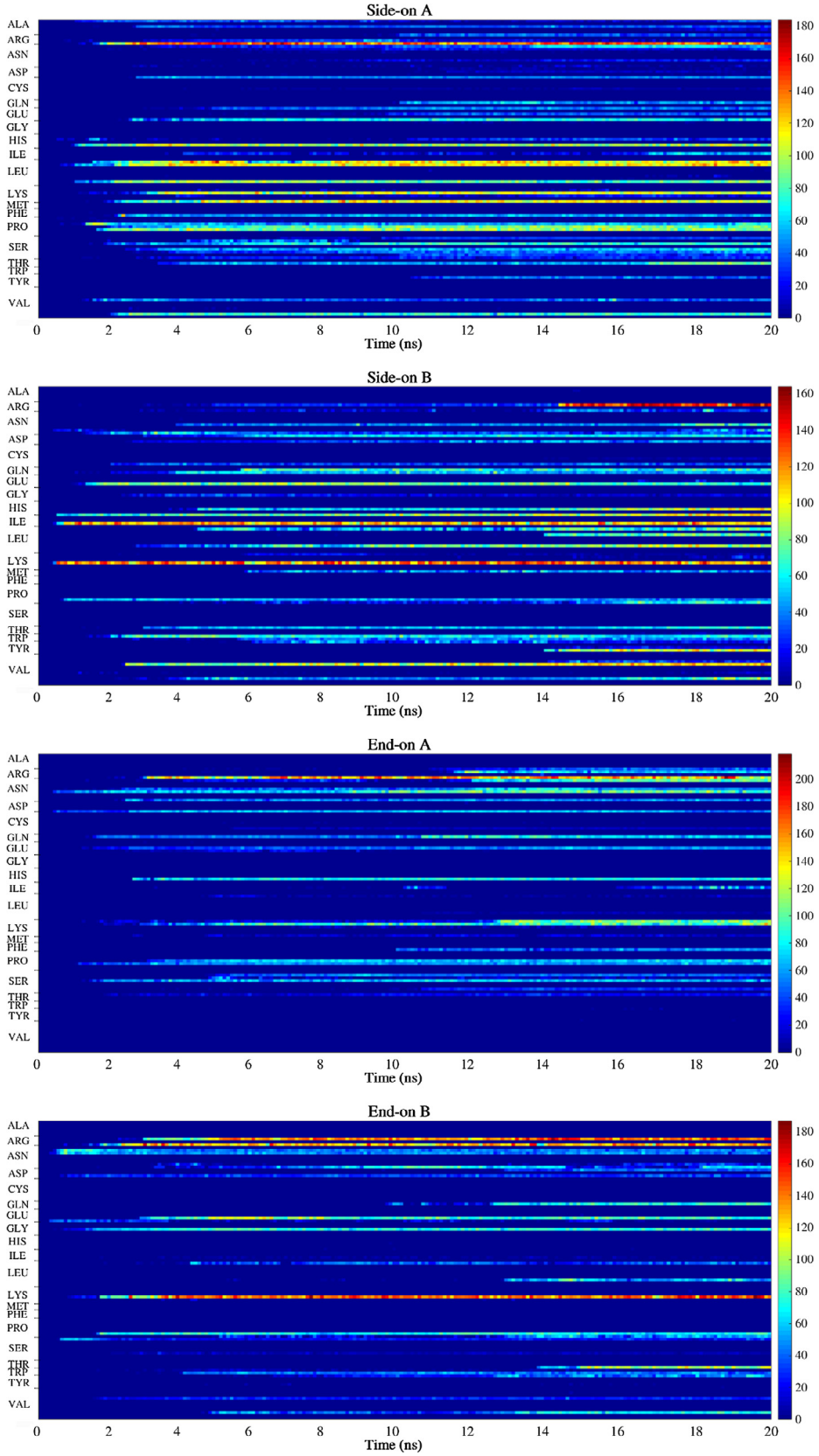

Fig. 7. Number of contacts between residue atoms and silicon nitride substrate during 20 ns simulations.

Charged amino acids ARG9 and LYS97, and hydrophobic LEU10 are responsible for the stronger interaction with silicon nitride for the side-on A orientation. In the case of end-on orientation, the main interactions were contributed by charged amino acids ARG9, LYS11, and LYS101, and polar ASN59 (see Fig. 9).

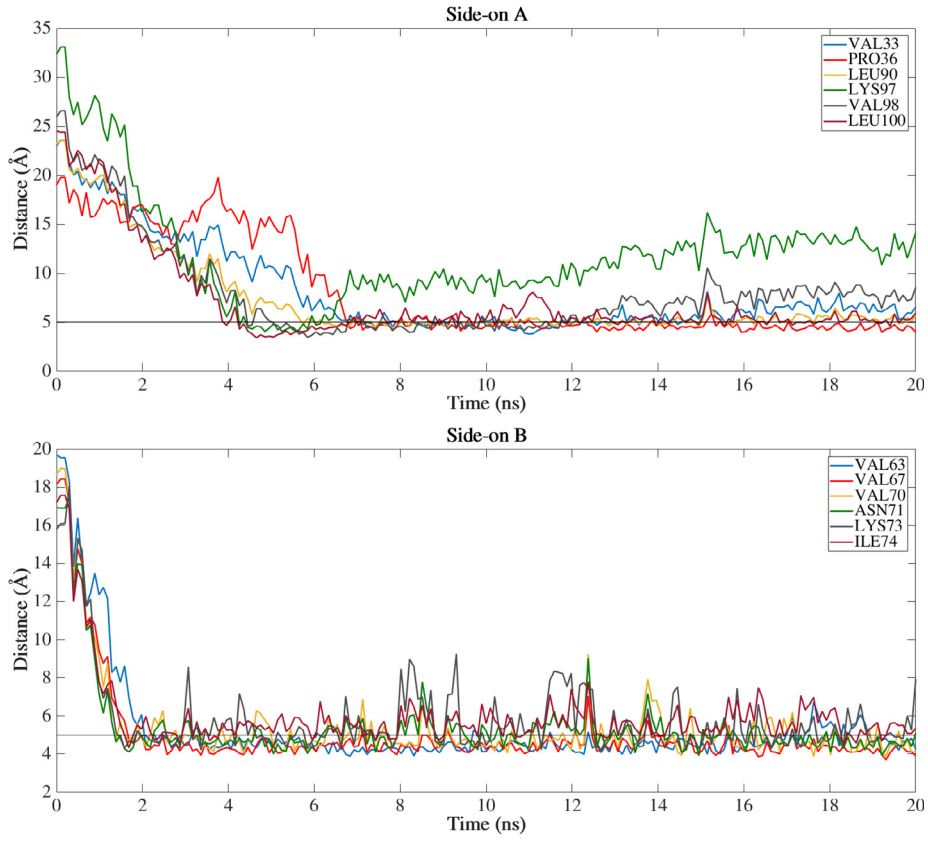

Fig. 8. Dominant residues that are within 5 Å of the gold surface.

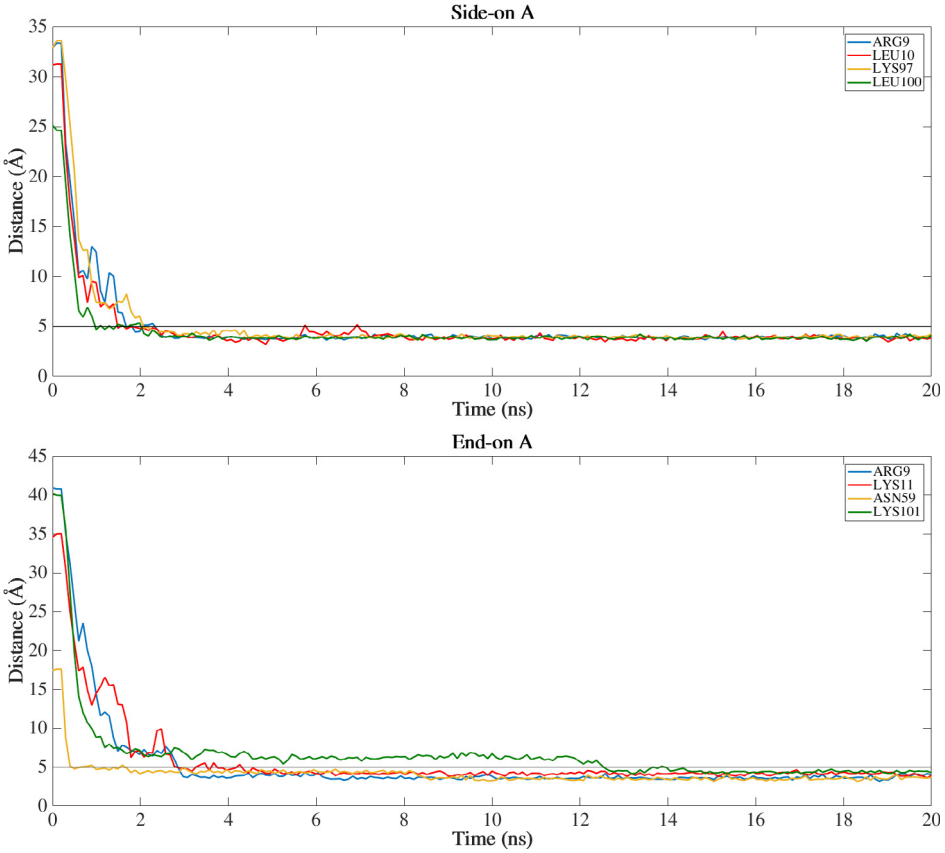

Fig. 9. Dominant residues that are within 5 Å of the silicon nitride surface.

4. Conclusion

This paper investigates the adsorption behavior of BMP-2 with four initial orientations on hydrophobic gold and hydrophilic silicon nitride. For all the simulations performed on gold, the water molecules constrained the movement of the protein within the drop restricting protein adsorption with the substrate. All the orientations of BMP-2 had their protein secondary structure preserved on the gold substrate. However, only weak Van der Waals interactions occurred, with mostly charged and hydrophobic residues which lay on the periphery of the drop surface. On most systems simulated, except end-on A, the protein adsorbed with a perpendicular orientation towards the surface, which was influenced by the arrangement of salt ions during the simulations.

On the silicon nitride substrate, strong adsorption occurred exclusively without direct contact between protein and surface via intermittent water layers. This strong adsorption is related to charge interactions and conformational change of the protein. The initial orientation of the protein strongly influenced the adsorption behavior. Simulations starting with side-on B and end-on B had at least three residues with more than 150 atoms adsorbing on the surface. This resulted in significant disruption of the β-sheet structures. Side-on A and End-on A also had strong binding to the Si_3N_4 surface and conserved their secondary structure. This might be related to the fact that only one residue (ARG9) had more than 150 atoms adsorbing on the surface.

End-on A orientation had less flexibility for spreading on both materials, with lower values of radius of gyration, which explains the late adsorption behavior on gold (after 14 ns). On silicon nitride, adsorption energy was lower with this orientation as compared to side-on A, which had the highest radius of gyration. Even with high values of radius of gyration (around 20.5 Å), this system with side-on A initial orientation had most of its secondary structure preserved.

BMP-2 adsorption is a strong function of the three-way interaction between the protein, the dissolution media, and the substrate. The salt ions play a vital role in the adsorption phenomenon. The dissolution media limited the adsorption on gold due to the high interaction of polar residues in the protein with the water molecules. The side-on A and end-on A orientations had strong adsorption with the silicon nitride without disruptions to their secondary structure. This research lays the foundation for identifying combinations of appropriate BMP-2 orientations with hydrophobic and hydrophilic substrates for medical applications.

Acknowledgment

This work was funded by US National Science Foundation (NSF CMMI: Award 1663128). In addition, we would like to thank CNPq (National Council for Scientific and Technological Development - Brazil) for the “Science without Borders” fellowship.

References

[1] M. Agashe, V. Raut, S.J. Stuart, R.A. Latour, Langmuir 21 (2005) 1103.
[2] M.R. King, Principles of Cellular Engineering: Understanding the Biomolecular Interface, Elsevier Academic Press, Amsterdam, 2006.
[3] T. Utesch, G. Daminelli, M.A. Mroginski, Langmuir 27 (2011) 13144.
[4] C. Mücksch, H.M. Urbassek, Langmuir 32 (2016) 9156.
[5] C. Mücksch, H.M. Urbassek, PLoS One 8 (2013) e64883.
[6] M. Beederman, J.D. Lamplot, G. Nan, J. Wang, X. Liu, L. Yin, R. Li, W. Shui, H. Zhang, S.H. Kim, J. Biomed. Sci. Eng. 6 (2013) 32.
[7] A.F. Oliveira, S. Gemming, G. Seifert, Materialwiss. Werkstofftech. 41 (2010) 1048.
[8] P.C. Bessa, M. Casal, R. Reis, J. Tissue Eng. Regen. Med. 2 (2008) 81.
[9] B. Huang, Y. Yuan, T. Li, S. Ding, W. Zhang, Y. Gu, C. Liu, Sci. Rep. 6 (2016) 24323.
[10] D.R. Schmidt, H. Waldeck, W.J. Kao, Biological Interactions on Materials Surfaces, Springer, 2009, p. 1.
[11] S. Al-Karadaghi, The 20 amino acids and their role in protein structures, Structural bioinformatics, protein crystallography, sequence analysis & homolog modeling.
[12] M. Ozboyaci, D.B. Kokh, R.C. Wade, Phys. Chem. Chem. Phys. 18 (2016) 10191.
[13] C. Mücksch, H.M. Urbassek, Chem. Phys. Lett. 510 (2011) 252.
[14] J.-W. Shen, T. Wu, Q. Wang, H.-H. Pan, Biomaterials 29 (2008) 513.
[15] B.S. Bal, M.N. Rahaman, Acta Biomater. 8 (2012) 2889.
[16] K. Mediaswanti, C. Wen, E.P. Ivanova, C.C. Berndt, V.T. Pham, F. Malherbe, J. Wang, Int. J. Surf. Sci. Eng. 8 (2014) 255.
[17] I.V. Likhachev, N.K. Balabaev, O.V. Galzitskaya, Open Biochem. J. 10 (2016) 1.
[18] J.Y. Jo, S.I. Jeong, Y.M. Shin, S.S. Kang, S.E. Kim, C.M. Jeong, J.B. Huh, Int. J. Oral Maxillofac. Surg. 44 (2015) 921.
[19] C. Strobel, N. Borman, A. Kadow-Romacker, G. Schmidmaier, B. Wildemann, J. Controlled Release 156 (2011) 37.
[20] B.-B. Seo, H. Choi, J.-T. Koh, S.-C. Song, J. Controlled Release 209 (2015) 67.
[21] O.P. Gautschi, S.P. Frey, R. Zellweger, ANZ J. Surg. 77 (2007) 626.
[22] S. Razzouk, R. Sarkis, N. Y. State, Dent. J. 78 (2012) 37.
[23] S. Tada, T. Kitajima, Y. Ito, Int. J. Mol. Sci. 13 (2012) 6053.
[24] N. Foloppe, A.D. MacKerell Jr, J. Comput. Chem. 21 (2000) 86.
[25] J.C. Phillips, R. Braun, W. Wang, J. Gumbart, E. Tajkhorshid, E. Villa, C. Chipot, R. D. Skeel, L. Kale, K. Schulten, J. Comput. Chem. 26 (2005) 1781.
[26] H.M. Berman, J. Westbrook, Z. Feng, G. Gilliland, T.N. Bhat, H. Weissig, I.N. Shindyalov, P.E. Bourne, Nucleic Acids Res. 28 (2000) 235.
[27] I. Marquetti, S. Desai, Molecular modeling of biochemical cues using high performance GPU, in: Proceedings of International Interdisciplinary Conference on Engineering Science & Management, Goa, India, 2016.
[28] A.F. Oliveira, S. Gemming, G. Seifert, J. Phys. Chem. B 115 (2011) 1122.
[29] M. Rabe, D. Verdes, S. Seeger, Adv. Colloid Interface Sci. 162 (2011) 87.
[30] A.D. MacKerell Jr, D. Bashford, M. Bellott, R.L. Dunbrack Jr, J.D. Evanseck, M.J. Field, S. Fischer, J. Gao, H. Guo, S. Ha, J. Phys. Chem. B 102 (1998) 3586.
[31] R. Braun, M. Sarikaya, K. Schulten, J. Biomater. Sci. Polym. Ed. 13 (2002) 747.
[32] J.R. Comer, D.B. Wells, A. Aksimentiev, in: DNA Nanotechnology: Methods and Protocols, Humana Press, Totowa, NJ, 2011, p. 317.
[33] I. Marquetti, S. Desai, Molecular Modeling of Bone Morphogenetic Protein for Tissue Engineering Applications Institute of Industrial and Systems Engineers Annual Conference, In Press, Florida, 2018.
[34] J. Cordeiro, S. Desai, J. Micro Nano-Manuf. 4 (2016) 041001.
[35] J. Cordeiro, S. Desai, J. Micro Nano-Manuf. 5 (2017) 031008.
[36] S. Desai, R.D. Kaware, J. Rodrigues, J. Nanoeng. Nanomanuf. 4 (2014) 237.
[37] S. Desai, R.D. Kaware, Int. J. Nanomanuf. 10 (2014) 432.
[38] K. Christmann, IMPRS-Lect. Ser. (2012).
[39] E.A. Vogler, Adv. Colloid Interface Sci. 74 (1998) 69.
[40] T.R. Kyriakides, Host Response to Biomaterials, Academic Press, Oxford, 2015, p. 81.
[41] L.J. Smith, K.M. Fiebig, H. Schwalbe, C.M. Dobson, Fold Des. 1 (1996) R95.
[42] C. Scheufler, W. Sebald, M. Hülsmeyer, J. Mol. Biol. 287 (1999) 103.
[43] J. Klages, A. Kotzsch, M. Coles, W. Sebald, J. Nickel, T. Müller, H. Kessler, Biochemistry 47 (2008) 11930.
[44] D. Weber, A. Kotzsch, J. Nickel, S. Harth, A. Seher, U. Mueller, W. Sebald, T.D. Mueller, BMC Struct. Biol. 7 (2007) 6.
[45] A.H. Reddi, Nat. Biotechnol. 16 (1998) 247.